Redox Biology 52 (2022) 102289

Contents lists available at ScienceDirect

Redox Biology

journal homepage: www.elsevier.com/locate/redox

IP3R1/GRP75/VDAC1 complex mediates endoplasmic reticulum stress-mitochondrial oxidative stress in diabetic atrial remodeling

Ming Yuan [a,b,1], Mengqi Gong [a,c,1], Jinli He [a,1], Bingxin Xie [a], Zhiwei Zhang [a], Lei Meng [a], Gary Tse [a], Yungang Zhao [d], Qiankun Bao [a], Yue Zhang [a], Meng Yuan [a], Xing Liu [a], Cunjin Luo [e], Feng Wang [f], Guangping Li [a], Tong Liu [a,*]

[a] Tianjin Key Laboratory of Ionic-Molecular Function of Cardiovascular Disease, Department of Cardiology, Tianjin Institute of Cardiology, Second Hospital of Tianjin Medical University, Tianjin, 300211, PR China
[b] Key Laboratory of Cardiovascular Intervention and Regenerative Medicine of Zhejiang Province, Department of Cardiology, Sir Run Run Shaw Hospital, Zhejiang University School of Medicine, Hangzhou, China
[c] Department of Cardiology, The First Affiliated Hospital of Anhui Medical University, Hefei, China
[d] Tianjin Key Laboratory of Exercise Physiology and Sports Medicine, Department of Health & Exercise Science, Tianjin University of Sport, Tianjin, 300381, PR China
[e] School of Computer Science and Electronic Engineering, University of Essex, Colchester, CO4 3SQ, UK
[f] Department of Genetics, School of Basic Medical Sciences, Tianjin Medical University, Tianjin, 300070, PR China

ARTICLE INFO

Keywords:
Endoplasmic reticulum stress
IP3R1–GRP75–VDAC1 complex
Mitochondria
Diabetes
Atrial fibrillation

ABSTRACT

Rationale: Endoplasmic reticulum (ER) stress and mitochondrial dysfunction are important mechanisms of atrial remodeling, predisposing to the development of atrial fibrillation (AF) in type 2 diabetes mellitus (T2DM). However, the molecular mechanisms underlying these processes especially their interactions have not been fully elucidated.

Objective: To explore the potential role of ER stress–mitochondrial oxidative stress in atrial remodeling and AF induction in diabetes.

Methods and results: Mouse atrial cardiomyocytes (HL-1 cells) and rats with T2DM were used as study models. Significant ER stress was observed in the diabetic rat atria. After treatment with tunicamycin (TM), an ER stress agonist, mass spectrometry (MS) identified several known ER stress and calmodulin proteins, including heat shock protein family A (HSP70) member [HSPA] 5 [GRP78]) and HSPA9 (GRP75, glucose-regulated protein 75). *In situ* proximity ligation assay indicated that TM led to increased protein expression of the IP3R1–GRP75–VDAC1 (inositol 1,4,5-trisphosphate receptor 1–glucose-regulated protein 75–voltage-dependent anion channel 1) complex in HL-1 cells. Small interfering RNA silencing of GRP75 in HL-1 cells and GRP75 conditional knockout in a mouse model led to impaired calcium transport from the ER to the mitochondria and alleviated mitochondrial oxidative stress and calcium overload. Moreover, GRP75 deficiency attenuated atrial remodeling and AF progression in Myh6-Cre^{+}/$Hspa9^{flox/flox}$ + TM mice.

Conclusions: The IP3R1–GRP75–VDAC1 complex mediates ER stress–mitochondrial oxidative stress and plays an important role in diabetic atrial remodeling.

1. Introduction

Atrial fibrillation (AF) is the most common sustained cardiac arrhythmia of clinical significance, and its incidence is increasing worldwide owing in part to an aging population [1]. Several risk factors induce structural and electrical remodeling of the atria, increasing the risk of AF development [2]. For example, diabetes mellitus (DM) is an important cause [3,4]. Our group has previously studied the roles of oxidative stress and inflammation in atrial remodeling and AF in diabetic animals [5,6]. Antioxidant therapies (such as NADPH oxidase inhibitor [7] and thiazolidinediones [8]) have proven effective in preventing atrial remodeling. However, the efficacy of antioxidants in preventing and treating AF has not been effectively clinically [9]. To aid

* Corresponding author. Tianjin Key Laboratory of Ionic-Molecular Function of Cardiovascular Disease, Department of Cardiology, Tianjin Institute of Cardiology, Second Hospital of Tianjin Medical University, No. 23, Pingjiang Road, Hexi District, Tianjin, 300211, PR China.;
E-mail addresses: liutong@tmu.edu.cn, liutongdoc@126.com (T. Liu).
[1] These authors contributed equally to this work.

https://doi.org/10.1016/j.redox.2022.102289
Received 27 January 2022; Received in revised form 6 March 2022; Accepted 13 March 2022
Available online 21 March 2022

Nonstandard abbreviations and acronyms

AF	Atrial fibrillation
DM	Diabetes mellitus
ER	Endoplasmic reticulum
ERS	Endoplasmic reticulum stress
GRP75	Glucose-regulated protein 75
IP3Rs	Inositol 1,4,5-trisphosphate receptors
MAM	Mitochondria-associated ER membranes
MS	Mass spectrometry
4-PBA	4-phenyl butyric acid
PLA	in situ proximity ligation assay
T2DM	Type 2 diabetic
TM	Tunicamycin
UPR	Unfolded protein response
VDAC	Voltage-dependent anion channel

the identification of potential drug targets, recent research has focused on elucidating potential mechanistic pathways, such as those related to energy metabolism, cellular calcium handling, and electrical conduction [10,11].

The mitochondria and endoplasmic reticulum (ER) are interconnected organelles and form an endomembrane network. Alterations in ER homeostasis can cause the accumulation of unfolded or misfolded proteins in the ER lumen, a phenomenon known as ER stress (ERS). A wide range of cellular environments and events induce ERS, and include high glucose, dysregulated calcium levels or redox homeostasis [12]. Currently, ERS is a central feature of metabolic diseases such as T2DM (type 2 diabetes) at the molecular, cellular, and organismal levels [13]. Treatment with the chemical chaperone 4-phenyl butyric acid (4-PBA), which alleviates ERS, protected canine cardiomyocytes from electrical remodeling induced by atrial tachycardia pacing, and from subsequent AF progression [14]. However, the precise mechanism of ER stress causes atrial remodeling and atrial fibrillation is still unclear. An important question remains: is ER stress involved in mitochondrial oxidative stress and reactive oxygen species (ROS) production in the pathophysiology of diabetes?

The contact points through which ER communicates with the mitochondria are referred to as mitochondria-associated ER membranes (MAM) [15]. MAM are enriched in phospholipid and glycosphingolipid synthesis enzymes, and in chaperone proteins, which control protein transport and the propagation of calcium signals and other metabolites between these two organelles to maintain cellular bioenergetics and integrity [16,17]. Calcium can be released from the ER through the intracellular calcium release channels inositol 1,4,5-trisphosphate receptors (IP3Rs) and via voltage-dependent anion channels (VDACs) at the outer mitochondrial membrane (OMM), eventually transferring to the mitochondria [18]. Earlier studies have shown that VDAC1 is physically connected to IP3R1 through the MAM-associated glucose-regulated protein 75 (GRP75, or heat shock protein family A [HSP70] member 9 [HSPA9]). GRP75 directly regulates calcium transfer from the ER to the mitochondria [17]. Calcium signaling is central to heart function through its physiological role in excitation-contraction coupling and the detrimental impact of calcium overload during heart failure and ischemia/reperfusion (I/R) injury [19]. Calcium depletion in the ER and calcium overloading in mitochondria via the MAM can lead to increased ROS generation and ER dysfunction, triggering the opening of the mitochondrial permeability transition pores (mPTP) and resulting in cell death [20].

In the present study, we evaluated the effect of tunicamycin (TM)-induced ERS on cardiac function, cardiomyocyte ultrastructure, and mitochondrial function. Considering the central position of GRP75 at the ER–mitochondrial interface outlined earlier, we used GRP75 as a starting point to examine whether calcium transfer from the ER to the mitochondria via the IP3R1–GRP75–VDAC1 complex might play a role in mitochondrial calcium overload and subsequent cardiomyocyte death in a diabetic model. We provide data to show that blocking ERS with 4-PBA and silencing GRP75 via small interfering RNA (siRNA) in HL-1 cells and in a *Hspa9* conditional knockout mouse model inhibits calcium transport from the ER to the mitochondria and antagonizes mitochondrial oxidative stress and calcium overload. Our findings provide new ideas and interventional targets for preventing and treating diabetic AF.

2. Methods

The data that support the findings of this study are available from the corresponding author upon reasonable request. Detailed methods are available in the online-only Data Supplement. Please see the Major Resources Table in the Supplemental Materials.

2.1. Mass spectrometry (MS)

Peptides were separated from the HL-1 cells after drug treatment using reverse-phase liquid chromatography on an EASY-nLC 1000 system and directly sprayed into a Q Exactive mass spectrometer. Full MS spectra were scanned between 300 and 1800 m/z with a resolution of 70,000 at 200 m/z (AGC target 1e6, 50-ms maximum injection time). MS/MS fragments were generated by higher-energy collision–induced dissociation (HCD), and the fragmentation was performed with 27% normalized collision energy. MS2 spectra were acquired with 17,500 resolution. The isolation window was 2 m/z. Normalized collision energy was 30 eV; underfill was 0.1%.

2.2. Proximity Ligation In Situ Assay

The Duolink II in situ proximity ligation assay (PLA) (Olink Bioscience) enables evaluation of the proximity of two proteins and their potential interaction (<40 nm) as an individual fluorescent dot under microscopy. Cell fixation and permeabilization were performed similarly to that for the immunofluorescence experiment. Subsequent blocking, antibody hybridizations, proximity ligations, and detection were performed according to the manufacturers' recommendations. The cells were imaged under an Olympus IX81 laser scanning microscope, and signals were quantified using BlobFinder software and expressed as the percentage of blobs per nucleus as compared with the controls.

2.3. Animal model

The investigation conformed to the Guide for the Care and Use of Laboratory Animals by the US National Institutes of Health. The study protocols and use of animals were approved by the Experimental Animal Administration Committee of Tianjin Medical University.

2.4. Diabetic animals and treatment protocol

Adult male Sprague–Dawley rats aged 8 weeks (200 ± 20 g) were purchased from HuaFuKang Bioscience Co., Ltd. (Beijing, China). High-fat diet (HFD, 60 kcal% fat, 20 kcal% carbohydrate, 20 kcal% protein) and low-dose streptozotocin (STZ) were used to induce T2DM. After a 1-week normal chow diet, the rats were divided into two groups: control and HFD. The control group was fed normal chow diet and the HFD group was fed high-fat chow (H10060, Beijing HuaFuKang Bioscience Co., Ltd.). After 4 weeks, all animals were overnight-fasted; the HFD group was given a single tail vein injection of STZ (30 mg/kg; Sigma-Aldrich) dissolved in 0.1 M citrate buffer (pH 4.5), and the control group was injected with the same dose of citrate buffer vehicle. At 72 h following the STZ injection, the fasting blood glucose levels (FBG) were measured in the HFD group; induction of diabetes was considered successful if the rats had FBG >11 mmol/L, and were used in further

experiments. The rats were then divided into three groups: control (Con); type 2 DM (T2DM); 4-PBA (20 mg/kg/day, p.o.); all rats were treated for 8 weeks and underwent the subsequent experiments.

2.5. Generation of Myh6-Cre^{+}/Hspa9$^{flox/flox}$ mice

Conditional cardiomyocyte-specific *Hspa9* knockout mice were generated using the Cre/LoxP system. Hspa9$^{flox/flox}$ mice under C57BL/6J background were purchased from Cyagen Biosciences Inc. (Guangzhou, China). Myh6-Cre^{+} mice were also purchased from Cyagen Biosciences Inc., with a cardiac-specific promoter driving *Cre* expression specifically in cardiomyocytes. The cardiomyocyte-specific *Hspa9* knockout (Myh6-Cre^{+}/Hspa9$^{flox/flox}$) mice were generated by crossing female Myh6-Cre^{+}/Hspa9$^{flox/+}$ mice with male Hspa9$^{flox/flox}$ mice. Tamoxifen (20 mg/kg) in corn oil was administered via intraperitoneal (i.p.) injection to 8–12-week-old male mice continuously for 5 days to induce *Cre* expression. DNA was extracted from mouse tail tissue for PCR genotyping, and protein was extracted from mouse atrial tissue for expression analysis via western blotting. Littermate male Hspa9$^{flox/flox}$ mice were considered control mice. All mice were housed in temperature-controlled cages with a 12-h light–dark cycle, and given free access to water and food. To study ERS *in vivo*, the mice were given i.p. injection of TM (0.5 mg/kg dissolved by dimethyl sulfoxide [DMSO] and diluted by saline) or the equivalent volume of vehicle (saline, 0.9% w/v, control), once a week for 2 weeks. Echocardiographic parameters were assessed 2 weeks after injection, and the hearts were harvested for molecular studies.

2.6. Intracardiac programmed electrical stimulation

A standard 2-lead surface ECG was recorded for 5 min before surgery. The right jugular vein was isolated via a small opening of the skin on the frontal neck region, and a 1.1-F octapolar electrophysiology catheter was inserted and advanced to the right ventricle via the right atrium. Arrhythmia vulnerability was assessed using a modified protocol: Stimulation frequency of 40–20 ms (this time is the duration of a single stimulus), decreasing every 2 ms, S1–S1 continuous stimulation (no interval between two single stimuli) of 5 s, which was performed 5 times with 60-s intervals (depending on the appearance or duration of AF waveform set) at amplitude of 3 V. AF was defined as rapid, irregular atrial response of >1 s.

2.7. Statistical analysis

All data were expressed as the mean ± standard error of the mean (SEM). Each figure legends contains detailed information on sample size and data collection. Data were analyzed using either the two-tailed unpaired Student *t*-test or the non-parametric Mann-Whitney *U* test to compare means between the two experimental groups; analysis of variance (ANOVA) followed by the Bonferroni post-hoc test was used to compare means among multiple groups where appropriate; Chi-square test was used to analyze frequency data. Statistical analyses were performed using GraphPad Prism (Version 6; GraphPad Software, Inc., San Diego, CA, USA). $P < 0.05$ was considered statistically significant.

3. Results

3.1. ERS is upregulated in diabetic rats

To examine the presence or absence of ERS activation, ERS marker levels were examined in a T2DM rat model. A significant increase in the levels of the ERS proteins GRP78 (HSPA5) and CHOP was observed in the LA tissues of the T2DM group (Fig. 1A–D). Treatment with the ERS inhibitor 4-PBA in the diabetic rats prevented these changes. Another ERS protein, XBP1 (X-box binding protein 1), was not significantly increased in the T2DM group or 4-PBA group (Fig. 1E and F).

The representative echocardiographic images and hemodynamic images from the three rat groups are shown in Online Table II. Compared with the control group, the T2DM group had increased LAD (left atrial diameter), which was prevented by 4-PBA (Fig. 1G).

Hemodynamic studies showed that the +dp/dtmax was significantly increased in the T2DM group compared to the control group, and was partially rescued by 4-PBA ($P < 0.05$ vs. the T2DM group). No significant difference in SBP, DBP, MBP, or pulse pressure was observed between the three groups (Online Table II). Moreover, the P wave duration, PR interval, QRS duration, and QT and QTc intervals did not differ between the three groups (Online Table II).

The atrial electrophysiological studies (Online Table III) showed that there was no difference in the IACT (inter-atrial conduction time) or the AERP (atrial effective refractory period) between the three groups. A higher percentage of induced AF was observed for the T2DM group compared to the control (75% vs. 14.3%), and 4-PBA reduced this to 20% (Fig. 1H).

3.2. ERS mediated the IP3R1–GRP75–VDAC1 calcium channeling complex in the heart

To investigate the mechanisms of AF following increased ERS, the ERS inducer, TM, was applied to HL-1 cells. MS demonstrated many known ERS and calmodulin proteins (Fig. 2A), including GRP78, CaMKK2, and GRP75.

Given that the IP3R1–GRP75–VDAC1 complex directly controls calcium transfer from the ER to the mitochondria in rat liver and HeLa cells [17], we hypothesized that this complex plays a role in calcium exchange between the ER and the mitochondria, thereby contributing to AF induction. We next investigated the alterations of IP3R1/GRP75/VDAC1 protein levels in a rat model of type 2 diabetes. There was a significant increase in the MAM-enriched protein levels of IP3R1, GRP75, and VDAC1 in the LA tissues of the T2DM group (Online Figure IA, B).

Conventional immunofluorescence showed the colocalization of IP3R1, GRP75, and VDAC1 in the HL-1 cells, indicating that these proteins were good candidates for studying ER–mitochondria interactions (Fig. 2B). Moreover, in situ PLA was used to detect and quantify interactions between IP3R1 and VDAC1, two organelle surface proteins involved in the calcium channeling complex at the MAM.

As tethers of ~10 nm or ~25 nm adjoin the two organelles, depending on whether the smooth and/or rough ER is implicated [21], we hypothesized that the ER–mitochondria junction would enable proximity ligation and subsequent detection by hybridization of Texas Red–labeled oligonucleotide probes. Each fluorescent dot represented the formation of one IP3R1–VDAC1 interaction, allowing quantification of in situ ER–mitochondria interactions in individual cells. Similar in situ PLA experiments were also performed with the IP3R1–GRP75 and GRP75–VDAC1 antibody pairs. Investigation of the interactions between endogenous IP3R1–VDAC1, IP3R1–GRP75, or GRP75–VDAC1 proteins in fixed TM-treated HL-1 cells showed that fluorescent signals were enhanced for all protein pairs (Fig. 2C and D). These findings confirm the IP3R1–GRP75–VDAC1 complex in HL-1 cells, and that TM leads to increased protein expression of the IP3R1–GRP75–VDAC1 complex.

3.3. GRP75 controls calcium transfer from the ER to the mitochondria

Szabadkai et al. [17] suggested that GRP75 has a central role in establishing the protein complex with IP3R and VDAC, suggesting the scaffolding, rather than chaperoning, function of GRP75 in the complex. This led us to hypothesize that GRP75 would play an important role in calcium exchange between the ER and the mitochondria. siRNA knockdown of GRP75 downregulated GRP75 mRNA levels and protein expression (Fig. 3A–C). GRP78 and CHOP protein expression and mRNA levels were also detected (Online Figure IIA-D). GRP78 and CHOP protein expression and mRNA levels were substantially increased after TM treatment compared with the control; GRP75 downregulation did not

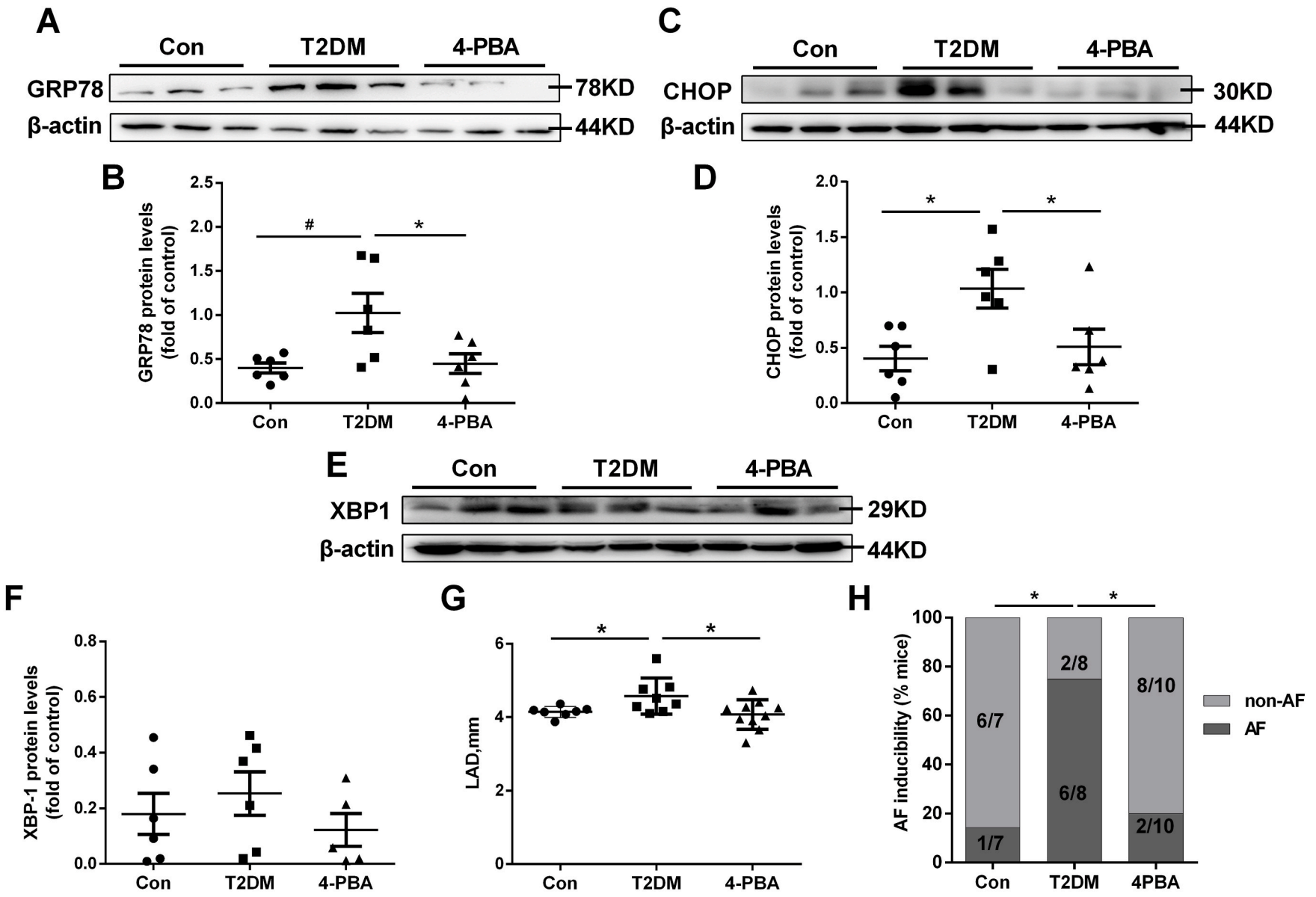

Fig. 1. Endoplasmic reticulum stress (ERS) is upregulated in type 2 diabetic rats and diabetic humans with atrial fibrillation (AF).

A–H, Rat model of type 2 diabetes by high-fat feeding + low-dose streptozotocin (STZ) injection with or without 4-phenyl butyric acid (4-PBA) for 8 weeks. Representative Western blot results and analysis of the protein expression in the three groups are shown. **A**, Western blot detection of GRP78 protein levels. **B**, Quantification of GRP78 protein levels in (**A**). **C**, Western blot detection of CHOP protein levels. **D**, Quantification of CHOP protein levels in (**C**). **E**, Western blot detection of XBP1 protein levels. **F**, Quantification of XBP1 protein levels in (**E**). Values are the mean ± SEM. n = 6 per group. $*P < 0.05$, $\#P < 0.01$, ANOVA with Bonferroni post-test. **G**, Analysis results of left atrial diameter (LAD). **H**, Quantification of the inducibility of AF. Values are the mean ± SEM. n = 7 in control group, n = 8 in T2DM group, n = 10 in 4-PBA group,. $*P < 0.05$, Chi-square test with Pearson's.

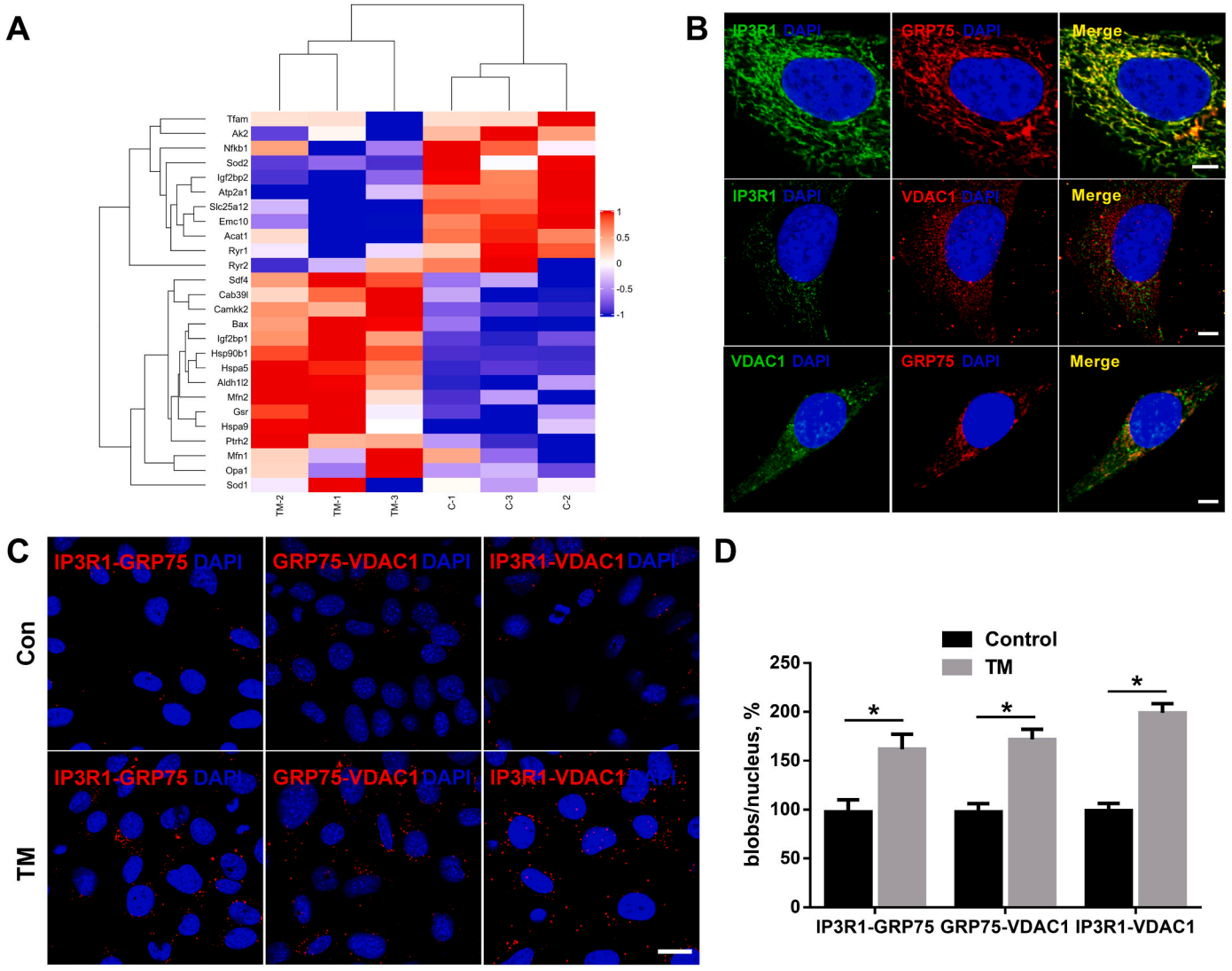

Fig. 2. The IP3R1–GRP75–VDAC1 complex plays an important role between the ER and the mitochondria in the heart.
A, HL-1 cells were cultured with tunicamycin (TM) for 24 h. Mass spectrometry identified GRP75 as a strong interacting protein. **B**, Conventional immunofluorescence confirming the colocalization of IP3R1, GRP75, and VDAC1 in HL-1 cells. Scale bar = 5 μm. **C**, **D**, In situ proximity ligation assay (PLA) monitoring of perturbation of ER–mitochondria interactions linked to genetic modulation of IP3R1–GRP75–VDAC1 complex proteins. Shown are representative PLA images (**C**) and quantitative analysis (**D**) of IP3R1–GRP75, GRP75–VDAC1, and IP3R1–VDAC1 interactions in HL-1 cells cultured with control or with TM for 24 h. Scale bar = 20 μm. Values are the mean ± SEM, n = 4 independent experiments, $^*P < 0.05$, two-tailed Student's *t*-test.

influence ERS significantly as compared with the TM group. It is an important insight that GRP75 knockdown does not affect the extent of ER stress, that this mechanism is downstream of ER stress response.

Recent studies have shown that ERS is related to IP_3 production and abnormal ER calcium release, which induces large increases in cytoplasmic calcium and mitochondrial calcium overloading. Accordingly, we examined cytoplasmic calcium using Fluo-4 staining. We found that the cytoplasmic calcium fluorescence intensity of the TM group was significantly higher than that in the control group (Fig. 3D and E). GRP75 downregulation did not significantly influence cytoplasmic calcium fluorescence intensity as compared with the TM group (Fig. 3D and E).

As a part of the mitochondrial network is closed to ER calcium release sites, calcium crosstalk between the ER and the mitochondria has been implicated in cardiomyocyte injury. Here, we explored the effect of ERS on mitochondrial calcium content. Mitochondrial calcium accumulation measured by Rhod-2 AM staining showed specific mitochondrial staining, overlapping with the mitochondrial marker Mito Tracker Green, and was significantly greater compared with that of the control group (Fig. 3F and G). By contrast, GRP75 downregulation was associated with reduced IP3R1–GRP75–VDAC1 interactions and mitochondrial calcium content as compared to the TM group. The protein expression of VDAC1 and MCU, which are located in the OMM and inner mitochondrial membrane (IMM), respectively, was detected. TM increased VDAC1 and MCU protein expression (Fig. 3H–J). siRNA downregulation of GRP75 expression led to a significant reduction in the amplitude of TM-stimulated increase of mitochondrial calcium relative to the TM group (Fig. 3H–J).

Together, these data suggest that inhibiting the IP3R1–GRP75–VDAC1 complex can prevent calcium transfer from the ER to the mitochondria during ERS and attenuate mitochondrial calcium overload.

3.4. Removing GRP75 from the ER–Mitochondria tether decreases the interactions within the two organelles

To determine the effects of ERS induction on the heart, ultrastructural analysis of HL-1 cardiomyocytes was carried out by transmission electron microscopy. An organized ER and uniformly sized and shaped

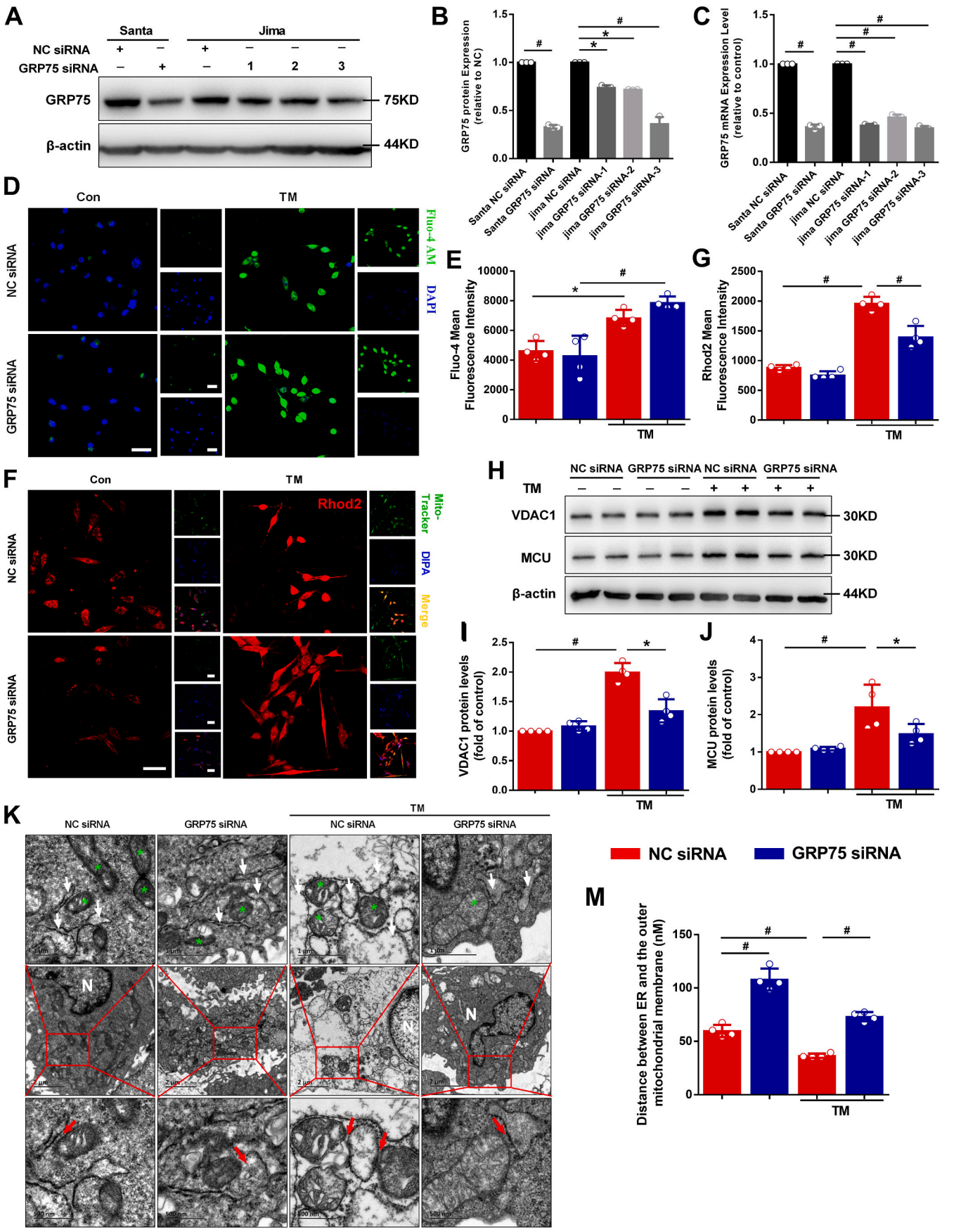

(caption on next page)

Fig. 3. GRP75 plays an important role in ER–mitochondria calcium exchange.
A, The silencing efficiency of GRP75 siRNAs; siRNAs from two companies (Santa Cruz Biotechnology [Santa] and Jima) were used for the experiment. **B**, Quantification of GRP75 protein levels in (**A**). **C**, Quantification of *GRP75* mRNA expression. **D**, Representative confocal microscopy images of fluorescence staining for Fluo-4 AM and DAPI. Scale bar = 20 μm. **E**, Quantification of Fluo-4 AM fluorescence intensity in (**D**). **F**, Representative confocal microscopy images of fluorescence staining for Rhod-2 AM and Mito Tracker Green. Scale bar = 20 μm. **G**, Quantification of Rhod-2 AM fluorescence intensity in (**F**). **H**, Western blot detection of mitochondria calcium protein VDAC1 and MCU levels in atrial myocytes. Quantification of VDAC1 (**I**) and MCU (**J**) protein levels in (**H**). **K**, Ultrastructural changes in HL-1 cells (green stars depict the mitochondria; white arrowheads depict the ER; red arrowheads depict ER–mitochondria contacts). N = Nucleus. Scale bars, top = 1 μm; middle = 2 μm; bottom = 500 nm. **M**, Measurements of ER–mitochondria interactions. Data are the mean ± SEM, n = 4 independent experiments, $^{*}P < 0.05$, $^{\#}P < 0.01$, ANOVA with Bonferroni post-test. (For interpretation of the references to colour in this figure legend, the reader is referred to the Web version of this article.)

mitochondria were observed in the negative control (NC) siRNA group (Fig. 3K). ERS induction with TM led to modification of the cardiomyocyte ultrastructure, as reflected by the dilatation and vesiculation of the ER, mitochondrial vacuolation, and mitochondrial cristae rupture. In the GRP75 siRNA-treated TM group, only partial dilatation and vesiculation of the ER and slight vacuolation of mitochondria were observed.

To investigate the ER–mitochondria interaction further, we analyzed the distance between the ER and the OMM. We found that the mean distance between the ER and the OMM was greater in the GRP75 siRNA group compared with the NC siRNA group. In the NC siRNA + TM group, the distance between the ER and the OMM was reduced during ERS, which is beneficial for calcium entry to the mitochondria through the ER, causing mitochondrial calcium overload. The ER–mitochondria distance at these sites was increased in the GRP75 siRNA + TM group (Fig. 3K–M), which reduced calcium entry into the mitochondria through the ER, thereby reducing mitochondrial calcium overload.

Together, our data indicate that the distance between the ER and the mitochondria increases in cells lacking GRP75, decreasing calcium transfer from the ER to the mitochondria and impairing mitochondrial calcium uptake.

3.5. Inhibiting GRP75 decreases ROS and improves the mitochondrial function of atrial myocytes

To elucidate the involvement of ROS in atrial ERS, we measured intracellular and mitochondrial ROS levels in HL-1 cells upon TM treatment using DCFH-DA and Mito Sox Red (Fig. 4A and C). TM increased the fluorescence intensity resulting from DCFH-DA and MitoSOX Red oxidation in the cells. GRP75 siRNA treatment decreased ERS-induced intracellular and mitochondrial ROS levels (Fig. 4A and B and 4C, D). The activity of Mn-SOD, a key enzyme in oxidative stress control, was reduced by TM-induced ERS (Fig. 4E and F). These results indicate that increased oxidative stress is observed in the HL-1 cells subjected to ERS and that the mitochondria may play an important role in this process.

ER calcium efflux and high levels of mitochondrial calcium accumulation are associated with the effects of several apoptosis signals. Destruction of the Δψm is widely considered to be one of the earliest events in the process of apoptosis. We detected the Δψm using JC-1. If Δψm loss or collapse occurred, the ratio of red–green fluorescence was reduced. After TM treatment, the dye remained mostly in the cytoplasm and emitted green fluorescence (Fig. 4G and H). In contrast, the dye in the GRP75 siRNA + TM group seemed to accumulate within the mitochondria and emitted red fluorescence.

As mitochondrial oxidative stress highly affects mitochondrial function, we sought to determine whether GRP75 is involved in the impact of mitochondrial functional capacity by TM in cardiomyocytes. GRP75 downregulation improved the TM-induced decrease in basal respiration (before oligomycin), maximum respiratory capacity (after FCCP), and ATPase-driven respiration (ΔOCR [oxygen consumption rate] basal-oligo) (Fig. 4I–L), suggesting that GRP75 mediates ERS-induced mitochondrial dysfunction.

3.6. Downregulation of GRP75 protects HL-1 cells from ERS-induced apoptosis

To examine whether ERS affects HL-1 cell survival, we performed flow cytometry assays. HL-1 cells were treated with TM for 24 h, and then stained with annexin V–FITC and PI and analyzed by flow cytometry. Compared with the control, TM significantly increased HL-1 cell apoptosis, and GRP75 siRNA markedly decreased TM-induced apoptosis (Fig. 5A). We investigated the expression levels of the apoptosis-related proteins in the cells via western blotting (Fig. 5B). ERS triggered apoptosis in the HL-1 cells by reducing the expression of Bcl-2 and caspase-3 while upregulating the expression of Bax and cleaved caspase-3 at protein level. After TM treatment, the cleaved caspase-9–caspase-9 ratio was also significantly increased in the HL-1 cells (Fig. 5B–E). Furthermore, the increased apoptosis observed after ERS was significantly attenuated in the GRP75 siRNA group.

Together, these results indicate that disrupting ER–mitochondria interaction via GRP75 tethering prevents ER–mitochondria calcium transfer during ERS and attenuates mitochondrial calcium loading and subsequent apoptosis.

3.7. GRP75 deficiency attenuates atrial remodeling and AF progression in mice

Finally, we utilized conditional cardiac-specific *Hspa9* knockout (Myh6-Cre^{+}/Hspa9$^{flox/flox}$) mice to confirm the role of GRP75. First, we assessed GRP75 expression in mouse heart via western blotting after treatment with tamoxifen to decrease cardiac GRP75 protein expression by ~80% (Fig. 6A). The representative echocardiographic, electrocardiographic, and hemodynamic images from the four groups are shown in Online Table V. For echocardiography data, LAD was not significantly different between the four experimental groups (Fig. 6C and D). Cardiac function as evaluated via the EF (Fig. 6E) and fractional shortening (Fig. 6F), and LV internal diameters in diastole and systole or wall thickness, was not affected by TM-induced ERS (Online Table IV). There was no significant difference in the SBP, DBP, MBP, and ±dp/dtmax between the four groups. The P wave duration, PR interval, and QRS duration were not significantly different between the four groups.

Atrial electrical conduction was recorded by activation mapping. The LA electrical conduction of the Hspa9$^{flox/flox}$ group was uniform and showed orderly spread to the surrounding tissue. However, in the Hspa9$^{flox/flox}$ + TM group, LA conduction was disordered, and there were abnormal conduction positions in the wave conduction, but it was restored in the Myh6-Cre^{+}/Hspa9$^{flox/flox}$ + TM group (Fig. 7A). The mapping images showed that LACV was significantly lower in the Hspa9$^{flox/flox}$ + TM group than in the Hspa9$^{flox/flox}$ group (0.39 ± 0.11 mm/ms vs. 1.02 ± 0.20 mm/ms, $P < 0.001$, Fig. 7B). This was partially improved in the Myh6-Cre^{+}/Hspa9$^{flox/flox}$ + TM group (0.65 ± 0.11 mm/ms vs. 0.39 ± 0.11 mm/ms, $P = 0.11$), although it did not reach statistical significance. LA conduction dispersion was higher in the Hspa9$^{flox/flox}$ + TM group than in the Hspa9$^{flox/flox}$ group (absolute, 11.33 ± 1.35 vs. 3.42 ± 0.96; index, 3.98 ± 0.67 vs. 1.37 ± 0.64, $P < 0.001$, Fig. 7C and D). By contrast, the dispersion of the Myh6-Cre^{+}/Hspa9$^{flox/flox}$ + TM group was reduced as compared with that of the Hspa9$^{flox/flox}$ + TM group.

The electrophysiological parameters obtained from intracardiac

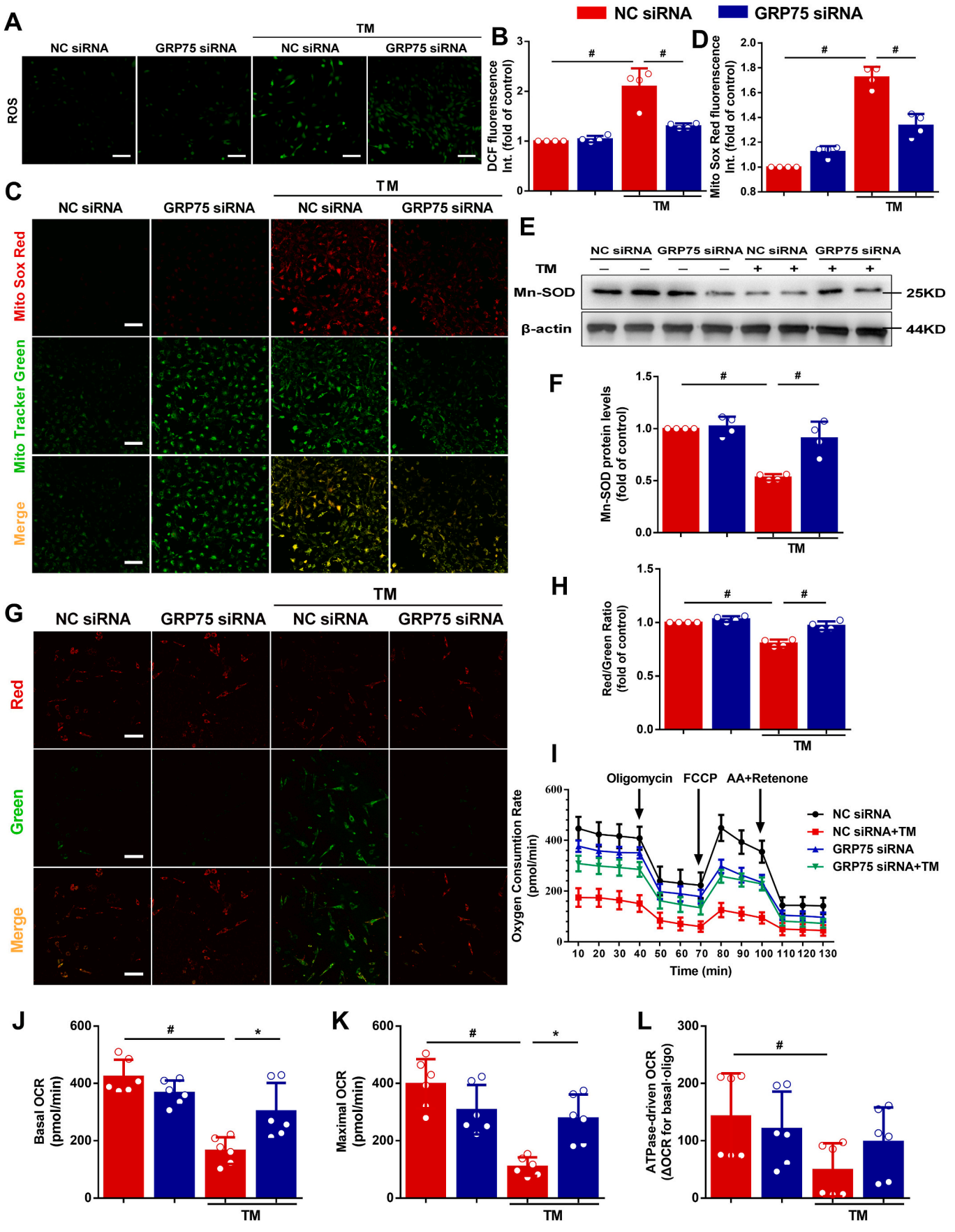

(caption on next page)

Fig. 4. Inhibiting GRP75 decreases reactive oxygen species (ROS) and improves mitochondrial function.
A, Confocal microscopy detection of HL-1 cells stained with 2′,7′-dichlorofluorescein diacetate (DCFH-DA). Scale bar = 100 μm. **B**, Quantification of ROS by DCFH-DA intensity in (**A**). **C**, Confocal microscopy detection of HL-1 cells stained with Mito Sox Red. Scale bar = 100 μm. **D**, Quantification of mitochondrial ROS by Mito Sox Red in (**C**). **E**, Western blot detection of antioxidant stress protein manganese superoxide dismutase (Mn-SOD) levels in atrial myocytes. **F**, Quantification of protein levels in (**E**). **G**, JC-1 staining. Scale bar = 100 μm. **H**, Quantification of mitochondrial membrane potential (Δψm) of HL-1 cells by JC-1 aggregate–monomer ratio. Data represent the mean ± SEM (n = 4 independent experiments), $^{\#}P < 0.01$, ANOVA with Bonferroni post-test. **I**, Analysis of oxygen consumption rate (OCR). Oligomycin inhibits ATP synthase (**J**), FCCP uncouples oxygen consumption from ATP production (**K**), and AA + Retenone inhibits complexes I and III (**L**). Data represent the mean ± SEM (n = 6 independent experiments), $^{*}P < 0.05$, $^{\#}P < 0.01$, ANOVA with Bonferroni post-test. . (For interpretation of the references to colour in this figure legend, the reader is referred to the Web version of this article.)

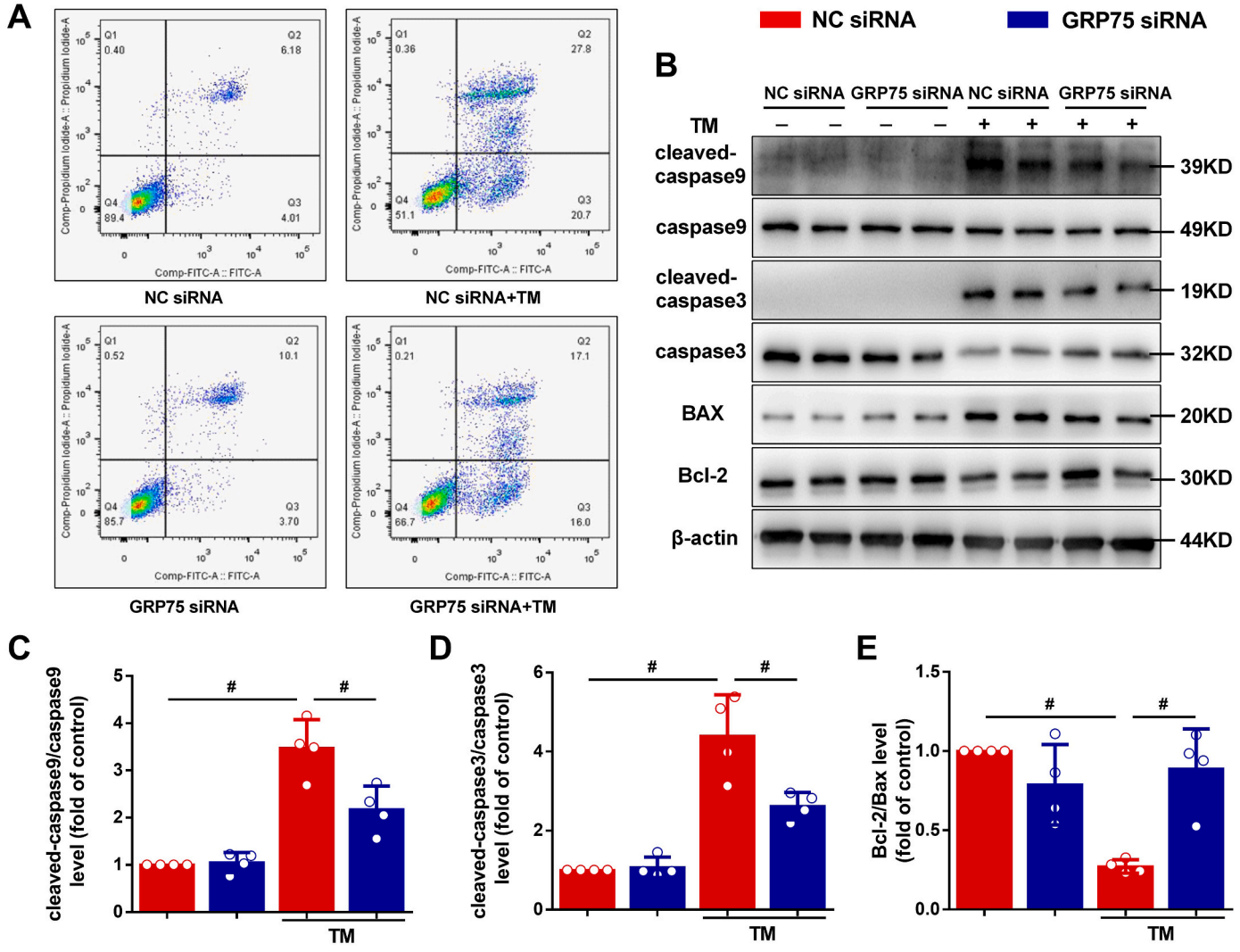

Fig. 5. Inhibition of GRP75 protects atrial myocytes from ERS-induced apoptosis.
A, HL-1 cells under 24-h TM stimulation. Apoptosis was evaluated by flow cytometry using annexin–V fluorescein isothiocyanate (FITC)/propidium iodide (PI) staining. **B–E**, GRP75 siRNA inhibited caspase-9 (**C**) and caspase-3 (**D**) activation and increased the Bcl-2–Bax ratio (**E**). Data are the mean ± SEM, n = 4 independent experiments, $^{\#}P < 0.01$, ANOVA with Bonferroni post-test.

programmed electrical stimulation showed no significant differences for the sinus cycle length (SCL) and AVWCL between the four groups (Fig. 7E). Compared to the Hspa9$^{flox/flox}$ group, SNRT was prolonged in the Hspa9$^{flox/flox}$ + TM group; in the Myh6-Cre^{+}/Hspa9$^{flox/flox}$ + TM group, SNRT was shortened as compared with the Hspa9$^{flox/flox}$ + TM group (Fig. 7F). We also measured the AERP in the 120-ms and 100-ms BCLs (Fig. 7G), the AERP in the Hspa9$^{flox/flox}$ + TM group were significantly decreased in the 120 ms compared with the Hspa9$^{flox/flox}$ group, which was attenuated by conditional cardiac-specific *Hspa9* knockout. We observed significantly higher AF incidence in the Hspa9$^{flox/flox}$ + TM group than in the Hspa9$^{flox/flox}$ group (63.6% vs. 9.1%, $P < 0.05$, Fig. 7H and I). AF was reduced in the Myh6-Cre^{+}/Hspa9$^{flox/flox}$ + TM group (18.2% vs. 63.6%, $P < 0.05$, Fig. 7I).

LA morphological changes were detected using HE and Masson's trichrome staining (Fig. 7J). Compared with the control group, increased inflammatory cell infiltration and extensive interstitial fibrosis of atrial cardiomyocytes were observed in the Hspa9$^{flox/flox}$ + TM group, and GRP75 knockout attenuated these changes (Fig. 7K).

Our results suggest that knockout of the key gene *GRP75* in the MAM improves ERS-induced atrial remodeling and reduces AF progression.

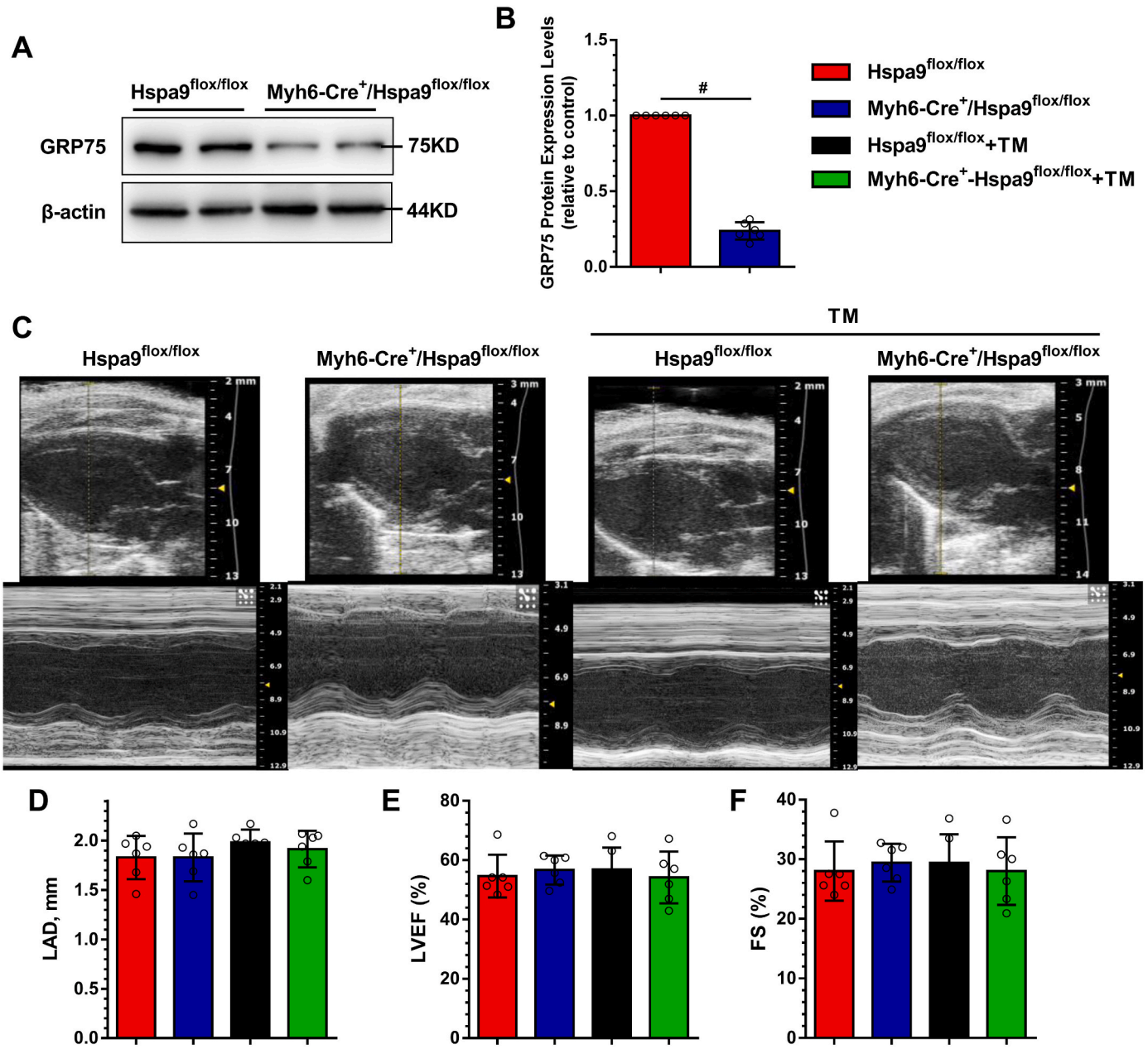

Fig. 6. Effect of GRP75 deficiency on echocardiography in TM-induced ERS mice.
A, Western blot assessment of GRP75 expression in mouse atria. **B**, Quantification of protein levels in (**A**). Data are the mean ± SEM, n = 6 per group, $^{\#}P < 0.01$, two-tailed unpaired Student's *t*-test. **C**, Representative 2D and M-mode echocardiographic images. Shown are analysis results of LAD (**D**), left ventricular ejection fraction (LVEF) (**E**), and fractional shortening (FS) (**F**). Data are the mean ± SEM, n = 6 per group, ANOVA with Bonferroni post-test.

4. Discussion

In the present study, we explored the interconnectivity and communication between the ER and the mitochondria in the pathological state of diabetes by establishing a diabetes model at the molecular, cellular, and system levels. Moreover, we investigated the molecular mechanisms involving the IP3R1–GRP75–VDAC1 complex and its effects on atrial remodeling, atrial cardiomyocyte apoptosis, and myocardial fibrosis. The main findings are: 1) the IP3R1–GRP75–VDAC1 complex mediates ERS–MAM–mitochondrial oxidative stress in diabetic atrial remodeling, and these changes are prevented by the ERS inhibitor, 4-PBA; and 2) gene silencing or knockout of the key gene *GRP75* of the MAM inhibits ER–mitochondrial calcium transport, alleviates mitochondrial oxidative stress, and prevents calcium overload, thereby preventing diabetic atrial remodeling (see Fig. 8).

Pulmonary veins and other ectopic triggers are the main initiators of AF occurrence, and atrial electrical and structural remodeling are important mechanisms of AF maintenance. Recent studies have shown that oxidative stress plays an important role in both AF occurrence and maintenance [22,23]. Here, we demonstrated an important role for ERS-associated mitochondrial oxidative stress in cardiomyocyte remodeling and AF progression using various pharmacological and genetic manipulations of the ERS pathway.

The ER is a specialized organelle that coordinates the synthesis, folding, and transport of at least one-third of the proteins in eukaryotic cells [12]. Disruption of ER homeostasis leads to the accumulation of unfolded or misfolded proteins and ERS, which activates the UPR, is activated as a compensatory pro-survival response to restore normal ER function. Three canonical UPR signaling pathways have been characterized: PRKR-like ER kinase (PERK)–eukaryotic translation initiation

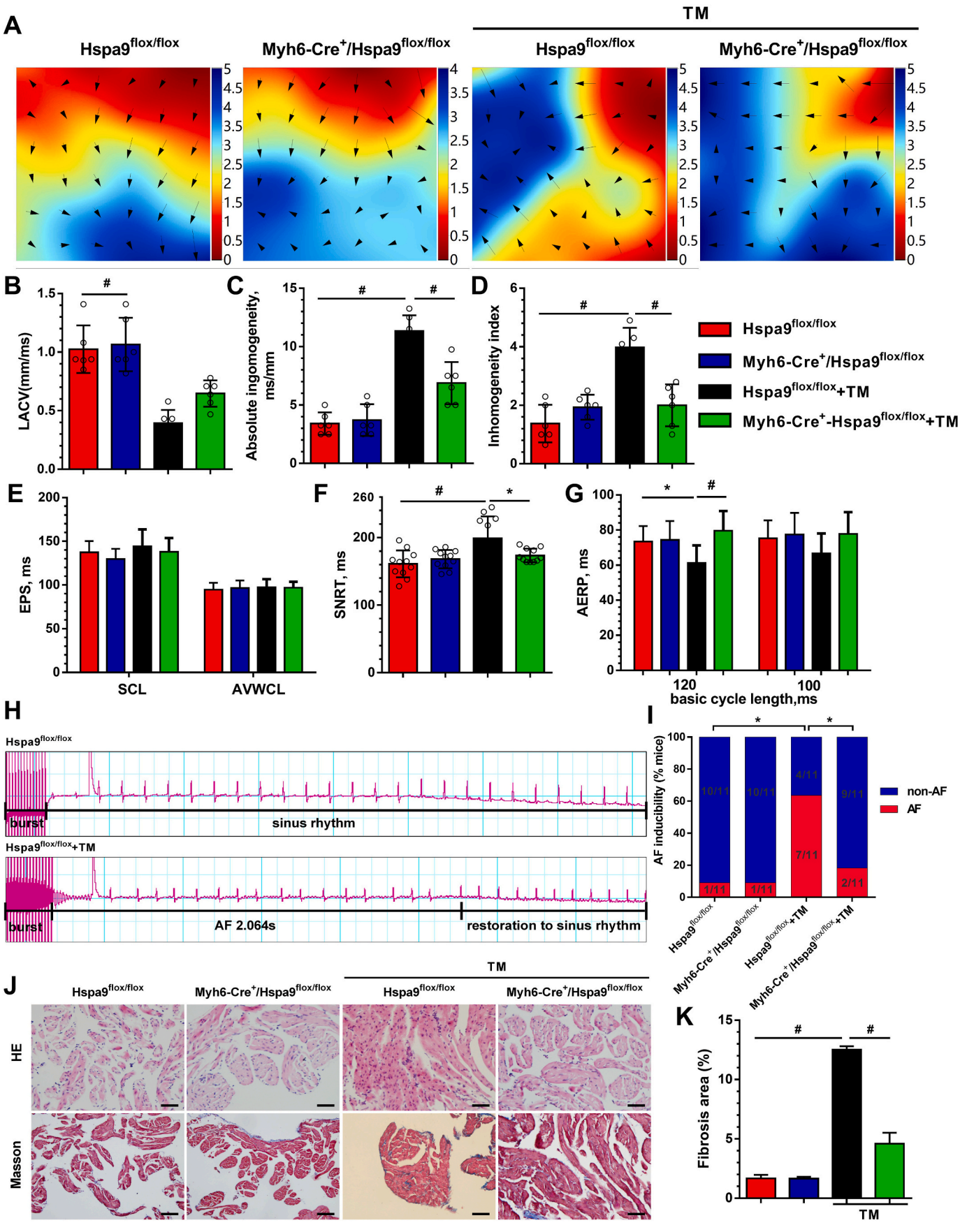

(caption on next page)

Fig. 7. Atrial remodeling and AF progression were attenuated in Myh6-Cre^{+}/Hspa9$^{flox/flox}$+ TM mice.
A, Epicardial electrical mapping recording of the left atria. Analysis results of left atrial conduction velocity (LACV) (**B**), LA absolute inhomogeneity (**C**), and LA inhomogeneity index (**D**), **B-D** data are the mean ± SEM, $^{\#}P < 0.01$, n = 6 per group, ANOVA with Bonferroni post-test. **E**, Analysis results of EPS parameters. SCL, sinus cycle length; AVWCL, atrioventricular Wenckebach cycle length. **F**, Quantifications of sinus node recovery time (SNRT). **G**, Quantification of atrium effective refractory period (AERP) at basic cycle lengths of 120 ms and 100 ms. **H**, Representative AF episodes induced by right atrial (RA) burst pacing. **I**, Quantification of AF inducibility. **E-I** values are the mean ± SEM. $^{*}P < 0.05$; $^{\#}P < 0.01$; n = 11 per group, Chi-square test with Pearson's. **J**, Representative images of RA HE and Masson's trichrome staining. Scale bar = 50 μm. **K**, Analysis results of interstitial fibrosis. Values are the mean ± SEM. $^{\#}P < 0.01$; n = 6 per group, ANOVA with Bonferroni post-test.

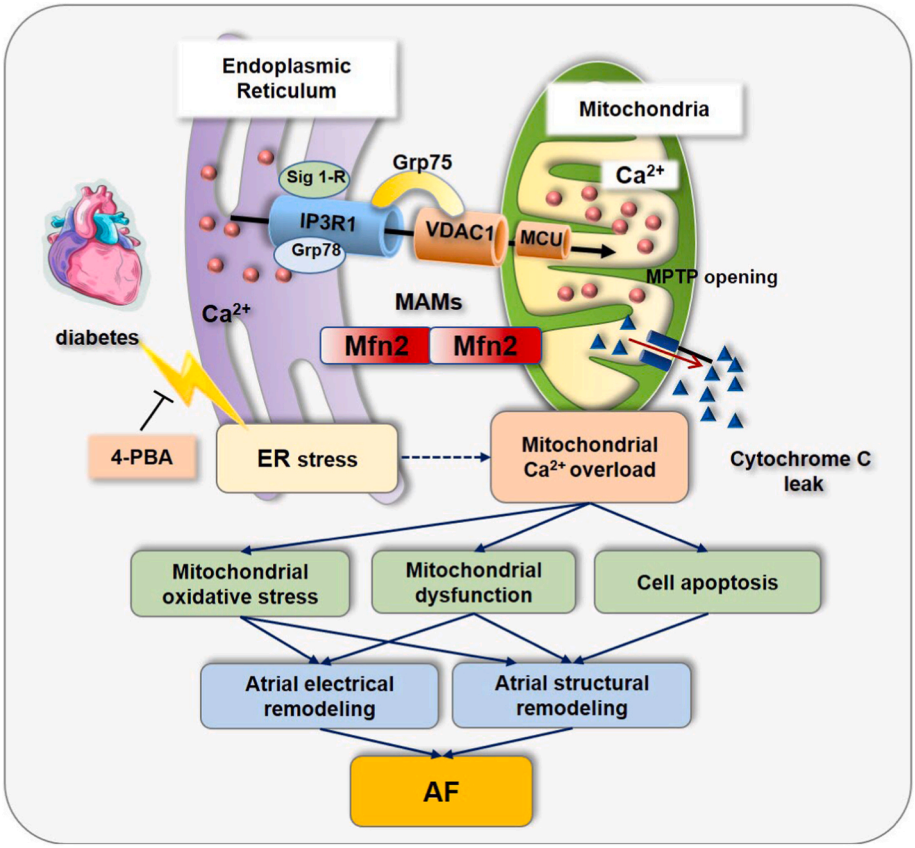

Fig. 8. The IP3R1–GRP75–VDAC1 complex mediates ERS–mitochondria-associated ER membranes (MAM)–mitochondrial oxidative stress and plays an important role in diabetic atrial remodeling.
Pharmacological prevention of ERS from upstream by the chemical chaperone 4-PBA precludes mitochondrial oxidative stress and improves atrial remodeling in diabetes. Gene silencing or knockout of the key gene *GRP75* of the MAMs inhibited ER–mitochondrial calcium transport, antagonizes mitochondrial oxidative stress and calcium overload, and improves diabetic atrial remodeling.

factor 2α (eIF2α), inositol-requiring protein 1α (IRE1α)–XBP1, and activating transcription factor (ATF)6α, which are normally kept inactive through the interaction with the ER resident chaperone GRP78/BIP1 [24]. Emerging evidence suggests that the three UPR signaling branches are not activated simultaneously; ATF6α and IRE1α activation occurs immediately and is attenuated with time through undefined mechanisms [25,26]. PERK activation follows that of ATF6α and IRE1α; prolonged UPR activation induces apoptosis, mainly through activation of the PERK–eIF2α–ATF4–CHOP pathway [25,26]. CHOP, encoded by the gene *DDIT3*, induces the expression of proapoptotic genes, such as *DR5*, *TRB3*, *BIM*, and *PUMA*, and represses the expression of the Bcl-2 family, together with direct calcium transfer from the ER to the mitochondria, which triggers mitochondrial apoptosis during ERS [27]. Our results demonstrate that using TM-induced ERS led to higher expression levels of the ERS markers GRP78 and CHOP in the cardiomyocytes. Furthermore, TM treatment resulted in reduced cardiac contractility and impaired intracellular calcium homeostasis. Under resting conditions in most cells, the steady-state ER calcium is 0.1–1 mM. The ER calcium ATPase (SERCA) pumps are crucial for maintaining ER calcium steady-state levels, coupling ATP hydrolysis with active transport of calcium from the cytosol back into the ER lumen, and the ER leak channels, such as the IP3Rs and the ryanodine receptors (RyRs). Chemical insults, and physiological or pathological stimuli are triggers that can cause a drop in ER luminal calcium, disrupting the folding machinery of the ER. The subsequent imbalance between the ER protein folding load and capacity will cause the accumulation of unfolded proteins in the ER lumen, engaging ERS. ERS further aggravates the depletion of calcium in the ER. In ER calcium disorder, the calcium in the ER is not only released into the cytoplasm, but also flows into the mitochondria through the MAM calcium channels, thereby affecting mitochondrial function and consequently energy metabolism [28]. Here, transmission electron microscopy analysis revealed that ERS-induced cardiac dysfunction is associated with important ultrastructural modifications in the HL-1 cells.

Recently, several MAM-specific proteins were identified, such as Mfn2, PACS2, and σ-1 receptor. Most of these proteins are ER proteins, with only a few (e.g., Mfn2) belonging to the mitochondria [29–31]. Here, we report that the enhanced interplay between the ER and the mitochondria in the atrial cells and the subsequent increased calcium flux from the ER to the mitochondria through the IP3R1–GRP75–VDAC1 complex may play important roles in atrial remodeling. In this manner, calcium is directly transferred from the ER lumen to the cytosol and across the OMM final transport into the mitochondrial matrix via the MCU [32,33]. The main physiological role of MCU-mediated mitochondrial calcium uptake is to balance energy supply and demand. Under pathological conditions such as I/R injury, MCU-mediated

mitochondrial calcium influx plays an important role in inducing mPTP opening and cell death [34]. IP_3R exists in three isoforms, and their subcellular distribution is cell-type dependent. IP_3R isoform 1 is highly expressed in the heart, but IP_3R isoform 2 is recognized as the predominant isoform in cardiac myocytes [35]. However, most of the functions of IP_3Rs are attributed to the type 1 isoform, and our results show that GRP75 interacts with IP_3R isoform 1. Likewise, the RyR, another calcium release channel, is also present at the MAM, and is the major calcium release channel on the sarcoplasmic reticulum (SR) in cardiomyocytes. In fact, accumulating evidence suggests that the IP3Rs are involved in cardiac calcium signaling, including excitation-contraction and excitation-transcription coupling [35–37]. In the present study, we validated an approach based on in situ PLA and immunocytofluorescence to detect and quantify ER–mitochondria interactions, and reveal that the MAM interface is an important novel player in regulating electrical and structural remodeling.

GRP75 modulates the lipopolysaccharide (LPS)-induced proinflammatory response and participates in many cellular functions such as stress response, intracellular trafficking, regulation of cell proliferation, and tumorigenesis [38,39]. GRP75 is a member of the HSP70 family of proteins, with a variety of biological functions, and is regarded not only as a molecular partner in MAM for regulating metabolism, but also interacts with many proteins to participate in the protective effect of stress reaction [40]. Following apoptosis of mouse podocytes induced by adriamycin or angiotensin II, it was confirmed that the expression of GRP75 was higher, the interaction between IP3R1-GRP75-VDAC1 complexes increased, mitochondrial Ca^{2+} overload and increased levels of cleaved caspase-3. While specific antagonists for GRP75 can prevent mitochondrial Ca^{2+} overload and podocyte apoptosis [41]. *In vitro*, the exposure of human bronchial epithelial cells to HMGB1 can significantly induce the expression of GRP75, enhanced ER-Mitochondrial Ca^{2+} transfer, ROS production and pro-inflammatory cytokine release. While HMGB1-induced these changes were attenuated by knockdown of GRP75 with GRP75 siRNA treatment [42]. Intriguingly, we found that GRP75 knockdown using siRNA significantly inhibited the effects of ERS, including the increase in ER–mitochondrial calcium transfer, and increased ROS production and apoptosis. Our results demonstrate that the association of the ER and mitochondria was decreased in *GRP75*-knockout cardiomyocytes, based on the reduced cardiomyocyte ER–mitochondrial contact length. These results suggest that calcium crosstalk between the ER and the mitochondria in cardiomyocytes plays an important role in atrial remodeling. In addition, several potential limitations of this article should be noted. Firstly, the number of experiments reported in some figures is low, we will increase this in future experiments. Secondly, there is a lack of key negative and positive controls in the experiments on $Hspa9^{flox/flox}$ mice.

5. Conclusion

The IP3R1–GRP75–VDAC1 complex mediates ERS–mitochondrial oxidative stress, playing an important role in diabetic atrial remodeling. Inhibiting GRP75 attenuates mitochondrial oxidative stress and calcium overload, increases the $\Delta\psi m$ and mitochondrial oxygen consumption, and protects cells from ERS-induced apoptosis. Knockout of GRP75 of the MAM improves ERS-induced atrial remodeling and reduces AF progression.

Sources of funding

National Natural Science Foundation of China (NSFC): T.L., 81970270; National Natural Science Foundation of China (NSFC): T.L., 81570298; National Natural Science Foundation of China (NSFC): Y.Z., 31971100; Tianjin Key Medical Discipline (Specialty) Construction Project.

Declaration of competing interest

None.

Acknowledgments

We acknowledge professor Zhenyi Ma in Tianjin Medical University for his guidance and support on Proximity Ligation In Situ Assay (PLA).

Appendix A. Supplementary data

Supplementary data to this article can be found online at https://doi.org/10.1016/j.redox.2022.102289.

References

[1] S.S. Chugh, R. Havmoeller, K. Narayanan, D. Singh, M. Rienstra, E.J. Benjamin, R. F. Gillum, Y.H. Kim, J.H. McAnulty, Z.J. Zheng, M.H. Forouzanfar, M. Naghavi, G. A. Mensah, M. Ezzati, C.J.L. Murray, Worldwide epidemiology of atrial fibrillation: a global burden of disease 2010 study, Circulation 129 (8) (2014) 837–847.
[2] L. Staerk, J.A. Sherer, D. Ko, E.J. Benjamin, R.H. Helm, Atrial fibrillation: epidemiology, pathophysiology, and clinical outcomes, Circ. Res. 120 (9) (2017) 1501–1517.
[3] X. Du, J. Dong, C. Ma, Is atrial fibrillation a preventable disease? J. Am. Coll. Cardiol. 69 (15) (2017) 1968–1982.
[4] D.H. Lau, S. Nattel, J.M. Kalman, P. Sanders, Modifiable risk factors and atrial fibrillation, Circulation 136 (6) (2017) 583–596.
[5] H. Fu, C. Liu, J. Li, C. Zhou, L. Cheng, T. Liu, G. Li, Impaired atrial electromechanical function and atrial fibrillation promotion in alloxan-induced diabetic rabbits, Cardiol. J. 20 (1) (2013) 59–67.
[6] C. Liu, H. Fu, J. Li, W. Yang, L. Cheng, T. Liu, G. Li, Hyperglycemia aggravates atrial interstitial fibrosis, ionic remodeling and vulnerability to atrial fibrillation in diabetic rabbits, Anadolu Kardiyol. Derg. 12 (7) (2012) 543–550.
[7] J. Qiu, J. Zhao, J. Li, X. Liang, Y. Yang, Z. Zhang, X. Zhang, H. Fu, P. Korantzopoulos, T. Liu, G. Li, NADPH oxidase inhibitor apocynin prevents atrial remodeling in alloxan-induced diabetic rabbits, Int. J. Cardiol. 221 (2016) 812–819.
[8] T. Liu, H. Zhao, J. Li, P. Korantzopoulos, G. Li, Rosiglitazone attenuates atrial structural remodeling and atrial fibrillation promotion in alloxan-induced diabetic rabbits, Cardiovasc. Ther. 2014 32 (4) (2014) 178–183.
[9] Q. Shao, P. Korantzopoulos, H. Fu, L. Ye, E. Liu, G. Xu, G. Li, T. Liu, Effects of probucol on left atrial remodeling in patients with paroxysmal atrial fibrillation, Int. J. Cardiol. 207 (2016) 117–119.
[10] M. Tadic, C. Cuspidi, Type 2 diabetes mellitus and atrial fibrillation: from mechanisms to clinical practice, Arch. Cardiovasc. Dis. 108 (4) (2015) 269–276.
[11] G. Tse, E.T.H. Lai, V. Tse, J.M. Yeo, Molecular and electrophysiological mechanisms underlying cardiac arrhythmogenesis in diabetes mellitus, 2016, J. Diabetes Res. (2016), 2848759-2848759.
[12] M. Wang, R.J. Kaufman, Protein misfolding in the endoplasmic reticulum as a conduit to human disease, Nature 529 (7586) (2016) 326–335.
[13] U. Ozcan, Q. Cao, E. Yilmaz, A.-H. Lee, N.N. Iwakoshi, E. Ozdelen, G. Tuncman, C. Görgün, L.H. Glimcher, G.S. Hotamisligil, Endoplasmic reticulum stress links obesity, insulin action, and type 2 diabetes, Science 306 (5695) (2004) 457–461.
[14] M. Wiersma, R.A.M. Meijering, X.-Y. Qi, D. Zhang, T. Liu, F. Hoogstra-Berends, O. C.M. Sibon, R.H. Henning, S. Nattel, B.J.J.M. Brundel, Endoplasmic reticulum stress is associated with autophagy and cardiomyocyte remodeling in experimental and human atrial fibrillation, J. Am. Heart Assoc. 6 (10) (2017), e006458.
[15] C. Lopez-Crisosto, C. Pennanen, C. Vasquez-Trincado, P.E. Morales, R. Bravo-Sagua, A.F.G. Quest, M. Chiong, S. Lavandero, Sarcoplasmic reticulum-mitochondria communication in cardiovascular pathophysiology, Nat. Rev. Cardiol. 2017 14 (6) (2017) 342–360.
[16] J.H. Ma, S. Shen, J.J. Wang, Z. He, A. Poon, J. Li, J. Qu, S.X. Zhang, Comparative proteomic analysis of the mitochondria-associated ER membrane (MAM) in a long-term type 2 diabetic rodent model, Sci. Rep. 7 (1) (2017) 2062.
[17] G. Szabadkai, K. Bianchi, P. Várnai, D. De Stefani, M.R. Wieckowski, D. Cavagna, A.I. Nagy, T. Balla, R. Rizzuto, Chaperone-mediated coupling of endoplasmic reticulum and mitochondrial Ca2+ channels, J. Cell Biol. 175 (6) (2006) 901–911.
[18] A. Danese, S. Patergnani, M. Bonora, M.R. Wieckowski, M. Previati, C. Giorgi, P. Pinton, Calcium regulates cell death in cancer: roles of the mitochondria and mitochondria-associated membranes (MAMs), Biochim. Biophys. Acta Bioenerg. 1858 (8) (2017) 615–627.
[19] X. He, X.-Y. Bi, X.-Z. Lu, M. Zhao, X.-J. Yu, L. Sun, M. Xu, W.G. Wier, W.-J. Zang, Reduction of mitochondria-endoplasmic reticulum interactions by acetylcholine protects human umbilical vein endothelial cells from hypoxia/reoxygenation injury, Arterioscler. Thromb. Vasc. Biol. 35 (7) (2015) 1623–1634.
[20] R.M.L. La Rovere, G. Roest, G. Bultynck, J.B. Parys, Intracellular Ca(2+) signaling and Ca(2+) microdomains in the control of cell survival, apoptosis and autophagy, Cell Calcium 60 (2) (2016) 74–87.
[21] G. Csordás, C. Renken, P. Várnai, L. Walter, D. Weaver, K.F. Buttle, T. Balla, C. A. Mannella, G. Hajnóczky, G. Hajnóczky, Structural and functional features and

significance of the physical linkage between ER and mitochondria, J. Cell Biol. 174 (7) (2006) 915–921.
[22] B.S. Karam, A. Chavez-Moreno, W. Koh, J.G. Akar, F.G. Akar, Oxidative stress and inflammation as central mediators of atrial fibrillation in obesity and diabetes, Cardiovasc. Diabetol. 16 (1) (2017) 120.
[23] T. Liu, G. Li, L. Li, P. Korantzopoulos, Association between C-reactive protein and recurrence of atrial fibrillation after successful electrical cardioversion: a meta-analysis, J. Am. Coll. Cardiol. 49 (15) (2007) 1642–1648.
[24] C. Hetz, F.R. Papa, The unfolded protein response and cell fate control, Mol. Cell. 69 (2) (2018) 169–181.
[25] J.H. Lin, H. Li, D. Yasumura, H.R. Cohen, C. Zhang, B. Panning, K.M. Shokat, M. M. Lavail, P. Walter, IRE1 signaling affects cell fate during the unfolded protein response, Science 318 (5852) (2007) 944–949.
[26] D.T. Rutkowski, S.M. Arnold, C.N. Miller, J. Wu, J. Li, K.M. Gunnison, K. Mori, A. A. Sadighi Akha, D. Raden, R.J. Kaufman, Adaptation to ER stress is mediated by differential stabilities of pro-survival and pro-apoptotic mRNAs and proteins, PLoS Biol. 4 (11) (2006) e374.
[27] I. Tabas, D. Ron, Integrating the mechanisms of apoptosis induced by endoplasmic reticulum stress, Nat. Cell Biol. 13 (3) (2011) 184–190.
[28] S.H. Back, R.J. Kaufman, Endoplasmic reticulum stress and type 2 diabetes, Annu. Rev. Biochem. 81 (2012) 767–793.
[29] O.M. de Brito, L. Scorrano, Mitofusin 2 tethers endoplasmic reticulum to mitochondria, Nature 456 (7222) (2008) 605–610.
[30] C. Giorgi, K. Ito, H.-K. Lin, C. Santangelo, M.R. Wieckowski, M. Lebiedzinska, A. Bononi, M. Bonora, J. Duszynski, R. Bernardi, R. Rizzuto, C. Tacchetti, P. Pinton, P.P. Pandolfi, PML regulates apoptosis at endoplasmic reticulum by modulating calcium release, Science 330 (6008) (2010) 1247–1251.
[31] T. Simmen, J.E. Aslan, A.D. Blagoveshchenskaya, L. Thomas, L. Wan, Y. Xiang, S. F. Feliciangeli, C.-H. Hung, C.M. Crump, G. Thomas, PACS-2 controls endoplasmic reticulum-mitochondria communication and Bid-mediated apoptosis, EMBO J. 24 (4) (2005) 717–729.
[32] J.M. Baughman, F. Perocchi, H.S. Girgis, M. Plovanich, C.A. Belcher-Timme, Y. Sancak, X.R. Bao, L. Strittmatter, O. Goldberger, R.L. Bogorad, V. Koteliansky, V. K. Mootha, Integrative genomics identifies MCU as an essential component of the mitochondrial calcium uniporter, Nature 476 (7360) (2011) 341–345.
[33] D. De Stefani, A. Raffaello, E. Teardo, I. Szabò, R. Rizzuto, A forty-kilodalton protein of the inner membrane is the mitochondrial calcium uniporter, Nature 476 (736) (2011) 336–340.
[34] E. Bertero, C. Maack, Calcium signaling and reactive oxygen species in mitochondria, Circ. Res. 122 (10) (2018) 1460–1478.
[35] E. Vermassen, J.B. Parys, J.-P. Mauger, Subcellular distribution of the inositol 1,4,5-trisphosphate receptors: functional relevance and molecular determinants, Biol. Cell. 96 (1) (2004) 3–17.
[36] P. Lipp, M. Laine, S.C. Tovey, K.M. Burrell, M.J. Berridge, W. Li, M.D. Bootman, Functional InsP3 receptors that may modulate excitation-contraction coupling in the heart, Curr. Biol. 10 (15) (2000) 939–942.
[37] H. Nakayama, I. Bodi, M. Maillet, J. DeSantiago, T.L. Domeier, K. Mikoshiba, J. N. Lorenz, L.A. Blatter, D.M. Bers, J.D. Molkentin, The IP3 receptor regulates cardiac hypertrophy in response to select stimuli, Circ. Res. 107 (5) (2010) 659–666.
[38] J. Bertrand, N. Tennoune, R. Marion-Letellier, A. Goichon, P. Chan, K. Mbodji, D. Vaudry, P. Déchelotte, M. Coëffier, Evaluation of ubiquitinated proteins by proteomics reveals the role of the ubiquitin proteasome system in the regulation of Grp75 and Grp78 chaperone proteins during intestinal inflammation, Proteomics 13 (22) (2013) 3284–3292.
[39] L.A. Volobouеva, J.F. Emery, X. Sun, R.G. Giffard, Inflammatory response of microglial BV-2 cells includes a glycolytic shift and is modulated by mitochondrial glucose-regulated protein 75/mortalin, FEBS Lett. 587 (6) (2013) 756–762.
[40] Q. Ran, R. Wadhwa, R. Kawai, S.C. Kaul, R.N. Sifers, R.J. Bick, J.R. Smith, O. M. Pereira-Smith, Extramitochondrial localization of mortalin/mthsp70/PBP74/GRP75, Biochem. Biophys. Res. Commun. 275 (1) (2000) 174–179.
[41] H. Xu, N. Guan, Y.L. Ren, Q.J. Wei, Y.H. Tao, G.S. Yang, X.Y. Liu, D.F. Bu, Y. Zhang, S.N. Zhu, IP3R-Grp75-VDAC1-MCU calcium regulation axis antagonists protect podocytes from apoptosis and decrease proteinuria in an Adriamycin nephropathy rat model, BMC Nephrol. 19 (1) (2018) 140.
[42] Y.H. Lv, Y.L. Li, D.D. Zhang, A.B. Zhang, W.H. Guo, S.F. Zhu, HMGB1-induced asthmatic airway inflammation through GRP75-mediated enhancement of ER-mitochondrial Ca2+ transfer and ROS increased, J. Cell. Biochem. 119 (5) (2018) 4205–4215.